PRAMANA — journal of physics | © Indian Academy of Sciences | Vol. 72, No. 1 January 2009 pp. 119–129

Neutrino oscillations: Present status and outlook

THOMAS SCHWETZ
Physics Department, Theory Division, CERN, CH-1211 Geneva 23, Switzerland
E-mail: schwetz@cern.in; schwetz@mpi-hd.mpg.de

Abstract. The status of neutrino oscillations from global data is summarized, with the focus on the three-flavour picture. The status of sterile neutrino oscillation interpretations of the LSND anomaly in the light of recent MiniBooNE results is also discussed. Furthermore, an outlook on the measurement of the mixing angle θ_{13} in the near term future, as well as prospects to discover CP violation in neutrino oscillations and to determine the type of the neutrino mass ordering by long-baseline experiments in the long term future are given.

Keyword. Neutrino oscillations.

PACS Nos 14.60.Lm; 14.60.Pq; 14.60.St

1. Global three-flavour analysis

Thanks to the spectacular developments in neutrino oscillation experiments in the last years we have now a rough picture of the parameters governing three-flavour oscillations: There are two mass-squared differences separated roughly by a factor 30, there are two large mixing angles (θ_{23}, which could even be 45°, and θ_{12}, which is large but smaller than 45° at very high significance), and one mixing angle which has to be small (θ_{13}). Present data is consistent with two possibilities for the neutrino mass ordering, conventionally parametrized by the sign of Δm^2_{31}: In the normal ordering ($\Delta m^2_{31} > 0$) the mass state which contains predominantly the electron neutrino has the smallest mass, whereas in the inverted ordering ($\Delta m^2_{31} < 0$) it is part of a nearly degenerate doublet of mass states, which is separated from the lightest neutrino mass by $|\Delta m^2_{31}|$.

In this section, an update on the determination of three-neutrino oscillation parameters from a global analysis of latest world neutrino oscillation data from solar, atmospheric, reactor, and accelerator experiments is presented. These results are based on work in collaboration with Maltoni, Tortola and Valle, published in [1,2] (see also the arXiv version 6 of [2] for updated results). The present determination of the three-flavour oscillation parameters is summarized in table 1, where the best fit points and the 2σ and 3σ allowed ranges are given.

This analysis includes latest data from the MINOS [3] and KamLAND [4,5] Collaborations which lead to an improved determination of the mass-squared

Table 1. Best-fit values, 2σ and 3σ intervals (1 d.o.f.) for the three-flavour neutrino oscillation parameters from global data including solar, atmospheric, reactor (KamLAND and CHOOZ) and accelerator (K2K and MINOS) experiments.

Parameter	Best fit	2σ	3σ
Δm^2_{21} (10^{-5}eV^2)	7.6	7.3–8.1	7.1–8.3
$\|\Delta m^2_{31}\|$ (10^{-3}eV^2)	2.4	2.1–2.7	2.0–2.8
$\sin^2\theta_{12}$	0.32	0.28–0.37	0.26–0.40
$\sin^2\theta_{23}$	0.50	0.38–0.63	0.34–0.67
$\sin^2\theta_{13}$	0.007	≤ 0.033	≤ 0.050

differences $|\Delta m^2_{31}|$ and Δm^2_{21}, respectively, mainly due to the precise spectral information. New MINOS data have been collected from June 2006 to July 2007 (Run-IIa), and they have been analysed together with the first data sample (Run-I), with a total exposure of 2.5×10^{20} p.o.t. In total, 563 ν_μ events have been observed at the far detector, while 738$\pm$30 events were expected for no oscillation. Recent KamLAND data [4] correspond to a total exposure of 2881 t·yr, almost four times larger than the 2004 data [5]. Apart from the increased statistics also systematic uncertainties have been improved: Thanks to the full volume calibration the error on the fiducial mass has been reduced from 4.7 to 1.8%. The main limitation for the Δm^2_{21} measurement comes now from the uncertainty on the energy scale of 1.5%. Details of our KamLAND analysis are described in Appendix A of [2]. We use the data binned in equal bins in $1/E$ to make optimal use of spectral information, and we take into account the (small) matter effect and carefully include various systematics. As previously, we restrict the analysis to the prompt energy range above 2.6 MeV to avoid large contributions from geo-neutrinos and backgrounds. In that energy range 1549 reactor neutrino events and a background of 63 events are expected without oscillations, whereas the observed number of events is 985.

Figure 1 illustrates how the determination of the leading 'solar' (θ_{12} and Δm^2_{21}) and 'atmospheric' (θ_{23} and $|\Delta m^2_{31}|$) oscillation parameters emerge from the complementarity of data from natural (Sun and atmosphere) and man-made (reactor and accelerator) neutrino sources. Spectral information from KamLAND data leads to an accurate determination of Δm^2_{21} with the remarkable precision of 5% at 2σ. KamLAND data also contribute to the lower bound on $\sin^2\theta_{12}$, whereas the upper bound is still dominated by solar data, most importantly by the CC/NC solar neutrino rate measured by SNO [6]. Moreover, as evident from figure 1 solar data fix the octant of θ_{12}, thanks to the MSW mechanism [7,8] due to matter effects inside the Sun, whereas the small matter effect in KamLAND cannot break the symmetry between the first and second θ_{12} octants.

We find a similar complementarity also in the determination of the atmospheric oscillation parameters (see the right panel in figure 1). In this case the $|\Delta m^2_{31}|$ determination is dominated by data from the MINOS long-baseline ν_μ disappearance experiment, which by now largely supersedes the pioneering K2K measurement [9], although in the global analysis the latter still contributes slightly to the lower bound on $|\Delta m^2_{31}|$. The determination of the mixing angle θ_{23} is dominated by atmospheric

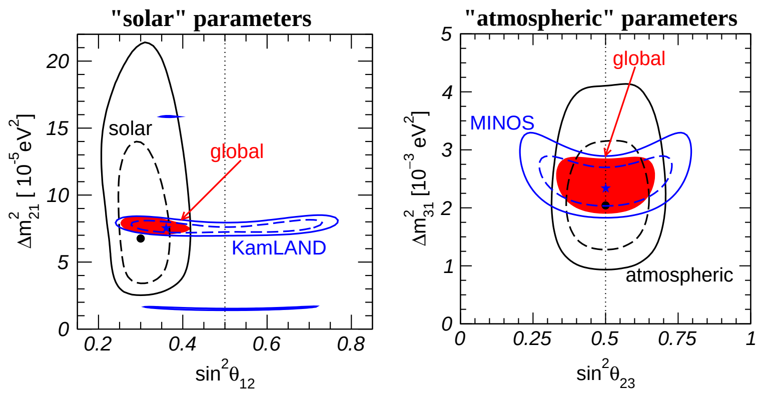

Figure 1. Determination of the leading 'solar' (left) and 'atmospheric' (right) oscillation parameters from the interplay of data from artificial and natural neutrino sources.

neutrino data from Super-Kamiokande [10], leading to a best fit point at maximal mixing [10a]. The sign of Δm^2_{31} (i.e., the neutrino mass hierarchy) is undetermined by the present data.

Similar to the case of the leading oscillation parameters, also the bound on θ_{13} emerges from an interplay of different data sets, as illustrated in figure 2. An important contribution to the bound comes, of course, from the CHOOZ reactor experiment [13] combined with the determination of $|\Delta m^2_{31}|$ from atmospheric and long-baseline experiments. However, due to a complementarity of low and high energy solar data, as well as solar and KamLAND data, solar+KamLAND provide a non-trivial constraint on θ_{13} (see [1,2,14]). We obtain at 90% CL (3σ) the following limits:

$$\sin^2\theta_{13} \leq \begin{cases} 0.051 \ (0.084) & \text{solar+KamLAND} \\ 0.028 \ (0.059) & \text{CHOOZ+atm+LBL} \\ 0.028 \ (0.050) & \text{global data} \end{cases} .$$

In the global analysis we find a slight weakening of the upper bound on $\sin^2\theta_{13}$ due to the new data from 0.04 (see [15] or v5 of [2]) to 0.05 at 3σ. The reason for this is two-fold. First, the shift of the allowed range for $|\Delta m^2_{31}|$ to lower values due to the new MINOS data implies a slightly weaker constraint on $\sin^2\theta_{13}$ (figure 1), and second, the combination of solar and new KamLAND data prefers a slightly non-zero value of $\sin^2\theta_{13}$ which, though not statistically significant, also results in a weaker constraint in the global fit. Note also that sub-leading effects in atmospheric neutrino data have an impact on the bound on θ_{13} at that level, as discussed in [15].

2. LSND and MiniBooNE results

Reconciling the LSND evidence [16] for $\bar{\nu}_\mu \to \bar{\nu}_e$ oscillations with the global neutrino data reporting evidence and bounds on oscillations remains a long-standing problem

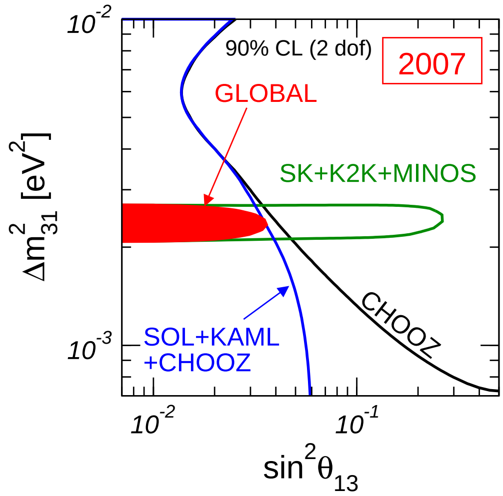

Figure 2. Constraint on θ_{13} from the global analysis of neutrino data.

for neutrino phenomenology. Recently, the MiniBooNE experiment [17] added more information to this question. This experiment searches for $\nu_\mu \rightarrow \nu_e$ appearance with a very similar L/E_ν range as LSND. No evidence for flavour transitions is found in the energy range where a signal from LSND oscillations is expected ($E > 475$ MeV), whereas an event excess is observed below 475 MeV at a significance of 3σ. Two-flavour oscillations cannot account for such an excess and currently the origin of this excess is under investigation. The exclusion contour from MiniBooNE is shown in figure 3 in comparison to the LSND allowed region and the previous bound from the KARMEN experiment [18], all in the framework of 2-flavour oscillations.

The standard 'solution' to the LSND problem is to introduce one or more sterile neutrinos at the eV scale in order to provide the required mass-squared difference to accommodate the LSND signal in addition to 'solar' and 'atmospheric' oscillations. However, in such schemes there is a severe tension between the LSND signal and short-baseline disappearance experiments, most importantly Bugey [19] and CDHS [20], with some contribution also from atmospheric neutrino data [21]. I report here the results from [22], where a global analysis including the MiniBooNE results has been performed in schemes with one, two and three sterile neutrinos.

Four-neutrino oscillations within the so-called (3+1) schemes have been only marginally allowed before the recent MiniBooNE results (see [2,23,24]), and become even more disfavoured with the new data, at the level of 4σ [22]. Five-neutrino oscillations in (3+2) schemes [24] allow for the possibility of CP violation in short-baseline oscillations [25]. Using the fact that in LSND the signal is in antineutrinos, whereas present MiniBooNE data are based on neutrinos, these two experiments become fully compatible in (3+2) schemes [22]. However, in the global analysis the tension between appearance and disappearance experiments remains unexplained. This problem is illustrated in figure 4 where sections through the allowed regions in the parameter space for the appearance and disappearance experiments are shown. An opposite trend is clearly visible: while appearance data require non-zero values

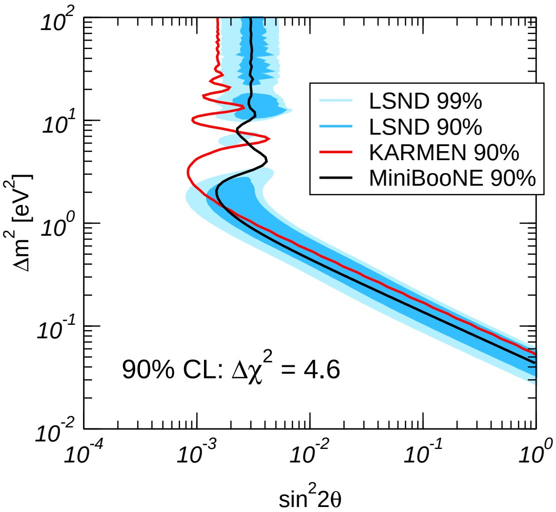

Figure 3. Exclusion contours at 90% (2 d.o.f.) for MiniBooNE and KARMEN compared to the LSND allowed region.

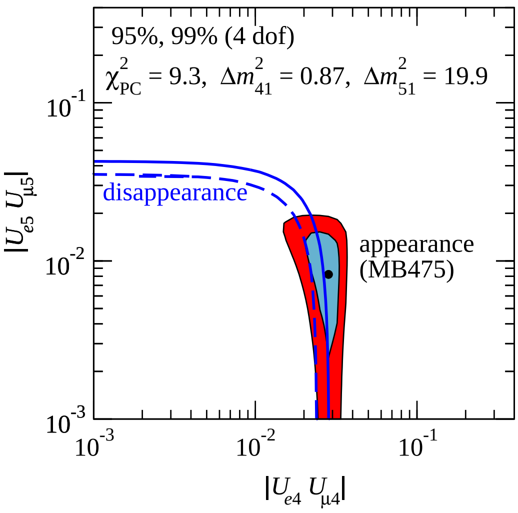

Figure 4. Section of the four-dimensional volumes allowed at 95% and 99% CL in the (3+2) scheme from SBL appearance and disappearance experiments in the space of the parameters in common to these two data sets. The values of Δm^2_{41} and Δm^2_{51} of the displayed sections correspond to the point in parameter space where the two allowed regions touch each other (at $\Delta\chi^2 = 9.3$).

for the mixing of ν_e and ν_μ with the eV-scale mass states four and five in order to explain LSND, disappearance data provide an upper bound on this mixing. The allowed regions touch each other at $\Delta\chi^2 = 9.3$, and a consistency test between these two data samples yields a probability of only 0.18%, i.e., these models can be considered as disfavoured at the 3σ level. Furthermore, when moving from four neutrinos to five neutrinos the fit improves only by 6.1 units in χ^2 by introducing four more parameters, showing that in (3+2) schemes the tension in the fit remains a severe problem.

Apart from grouping five neutrinos like (3+2) one can also consider the logical possibility of (1+3+1) ordering [26], where the three mass states responsible for solar and atmospheric oscillations are in between the lightest and heaviest mass states, both separated from the triplet by eV-scale mass differences. Such a scheme has a slightly different oscillation phenomenology as the (3+2) case considered in [22]. However, we have checked by explicit calculations that for (1+3+1) ordering also the conclusion of [22] is valid; no qualitatively new effects appear and the tension in the (1+3+1) fit is very similar to the (3+2) case. The (1+3+1) best fit point is found at

$$\begin{aligned} &U_{e4} = 0.12\,, \quad U_{e5} = 0.11\,, \quad U_{\mu 4} = 0.15\,, \quad U_{\mu 5} = 0.12\,, \\ &\delta = 0.89\pi\,, \quad \Delta m^2_{41} = -0.81\,\mathrm{eV}^2\,, \quad \Delta m^2_{51} = 1.1\,\mathrm{eV}^2\,, \end{aligned} \tag{1}$$

with $\chi^2_{\min} = 92.8$, compared to 94.5 for (3+2) [26a].

The tension in the fit remains a problem even in the case of three sterile neutrinos, since adding one more neutrino to (3+2) cannot improve the situation [22]; χ^2 decreases only by very few units at the price of introducing many more parameters. In [27], it is pointed out that an exotic sterile neutrino with energy-dependent mass or mixing can resolve these tensions. For an overview and references of exotic proposals to explain the LSND anomaly, see [28].

Currently, MiniBooNE is taking data with antineutrinos. This measurement is of crucial importance to test scenarios involving CP violation (such as (3+2) oscillations) to reconcile LSND and present MiniBooNE data. Therefore, despite the reduced flux and detection cross-section of antineutrinos, the hope is that enough data will be accumulated in order to achieve good sensitivity in the antineutrino mode. Furthermore, it is of great importance to settle the origin of the low energy excess in MiniBooNE. If this effect persists and does not find an 'experimental' explanation such as an overlooked background, an explanation in terms of 'new physics' seems to be extremely difficult. To the best of my knowledge, so far no convincing model able to account for the sharp rise with energy while being consistent with global data has been provided.

As discussed in the following section, the main goal of upcoming oscillation experiments like Double-ChOOZ, Daya Bay, T2K, NOνA is the search for the mixing angle θ_{13}, with typical sensitivities of $\sin^2 2\theta_{13} \gtrsim 1\%$ (figure 5). This should be compared to the size of the appearance probability observed in LSND: $P_{\mathrm{LSND}} \approx 0.26\%$. Hence, if θ_{13} is large enough to be found in those experiments sterile neutrinos may introduce some subleading effect, but their presence cannot be confused with a non-zero θ_{13}. Nevertheless, I argue that it could be worth to look for sterile neutrino effects in the next generation of experiments. They would introduce (mostly energy averaged) effects, which could be visible as disappearance signals in the near detectors of these experiments. This has been discussed [29] for the Double-CHOOZ experiment, but also the near detectors at superbeam experiments should be explored. An interesting effect of (3+2) schemes has been pointed out recently for high energy atmospheric neutrinos in neutrino telescopes [30]. The crucial observation is that for $\Delta m^2 \sim 1$ eV^2 the MSW resonance occurs around TeV energies, which leads to large effects for atmospheric neutrinos in this energy range, potentially observable at neutrino telescopes.

However, for the subsequent generation of oscillation experiments aiming at sub-per cent level precision to test CP violation and the neutrino mass hierarchy (see §4), the question of LSND sterile neutrinos is highly relevant [31,32]. They will lead to a miss-interpretation or (in the best case) to an inconsistency in the results. If eV scale sterile neutrinos exist with mixing relevant for LSND the optimization in terms of baseline and E_ν of high precision experiments has to be significantly changed. Therefore, I argue that it is important to settle this question at high significance before decisions on high precision oscillation facilities are taken.

3. Prospects for the near future

In the following, it is assumed that the LSND anomaly as well as the low energy MiniBooNE excess have a non-neutrino origin and hence, I stick to the standard three-flavour neutrino picture. Under these premises I try to give some outlook on developments in neutrino oscillations to be expected at a time scale of 5 to 10 years [33] (see also [34]). In this time-frame we expect results from a new generation of reactor experiments, Double-CHOOZ [35], Daya Bay [36], RENO [37], as well as the next generation of long-baseline superbeam experiments T2K [38] and NOνA [39].

The currently running MINOS experiment will improve further the determination of $|\Delta m^2_{31}|$ with accumulating statistics. Once results on ν_μ disappearance become available from the T2K and/or NOνA experiments a determination of this parameter at the level of a few per cent at 2σ will be obtained [33,38,39] (currently 12%, see table 1), and also $\sin^2\theta_{23}$ is likely to be measured with a precision better than the present atmospheric neutrino data.

Certainly, the main goal of the upcoming experiments is the determination of θ_{13}. Reactor experiments aim at this goal by exploring the disappearance of $\bar\nu_e$. The corresponding survival probability is given to very good accuracy by

$$P_{ee} = 1 - \sin^2 2\theta_{13} \sin^2 \frac{\Delta m^2_{31} L}{4E_\nu}\,. \tag{2}$$

This simple dependence shows that reactor experiments provide a clean measurement of $\sin^2 2\theta_{13}$, not affected by correlation or degeneracies with other unknown parameters [40]. The main issues in such an experiment are statistical and systematical errors, where the latter are going to be addressed by comparing data for near and far detectors. In contrast, the superbeam experiments look for the appearance of ν_e from a beam consisting initially mainly of ν_μ. At leading order in the small parameters $\sin 2\theta_{13}$ and $\tilde\alpha \equiv \sin 2\theta_{12}\Delta m^2_{21} L/4E_\nu$ the relevant oscillation probability (in vacuum, for simplicity) is

$$\begin{aligned} P_{\mu e} = {} & \sin^2 2\theta_{13}\, \sin^2\theta_{23}\, \sin^2\Delta + \tilde\alpha^2\, \cos^2\theta_{23} \\ & + \sin 2\theta_{13} \sin 2\theta_{23}\, \tilde\alpha \sin\Delta \cos(\Delta \pm \delta_{\rm CP})\,, \end{aligned} \tag{3}$$

where $\Delta \equiv \Delta m^2_{31} L/4E_\nu$ and '+' ('−') holds for neutrinos (antineutrinos). This expression shows that there is a complicated correlation of $\sin^2 2\theta_{13}$ with other

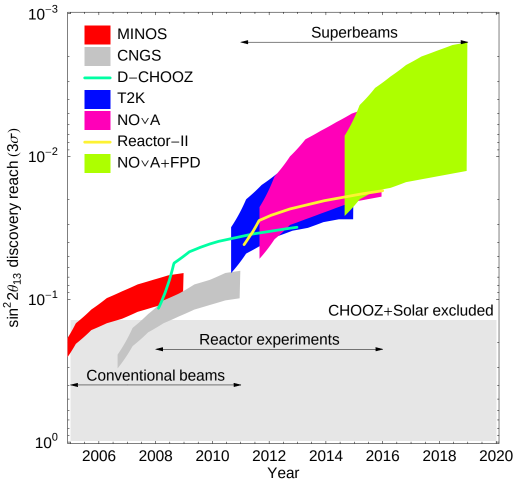

Figure 5. Evolution of the 3σ discovery potential of a non-zero value of θ_{13} of upcoming experiments (figure from [41]).

parameters, especially with the CP phase $\delta_{\rm CP}$. This effect is illustrated in figure 6, where the allowed region in the plane of $\sin^2 2\theta_{13}$ and $\delta_{\rm CP}$ is shown for T2K, NOνA, a reactor experiment, and the combination, assuming an input value of $\sin^2 2\theta_{13} = 0.1$ and $\delta_{\rm CP} = 90°$. For the superbeams the allowed regions show a typical 'S'-shape, reflecting the trigonometric dependence of the probability on $\delta_{\rm CP}$. Furthermore, solutions with the wrong mass hierarchy (gray curves in the figure) introduce another ambiguity in the interpretation. On the other hand, the figure shows that a reactor experiment can determine $\sin^2 2\theta_{13}$ unambiguously. The rightmost panel illustrates the situation which could emerge from the global analysis of these experiments: A relatively good determination of θ_{13}, some information on $\delta_{\rm CP}$ (though CP violation cannot be established), which however is largely corrupted by the ambiguity in the mass hierarchy, which cannot be resolved in this particular example ($\Delta\chi^2$ of the wrong hierarchy is only 3.1 in the global analysis).

Figure 5 shows the evolution of the θ_{13} discovery reach as a function of time, where of course a significant uncertainty is associated with the horizontal axis. The complementarity of beam and reactor experiments is also visible in that figure: The wide bands for the beam experiments follow from the impact of the (unknown) true value of $\delta_{\rm CP}$, which could be in favour for discovering a non-zero value of θ_{13} or not. In contrast, reactor experiments do not depend on the CP-phase and their reach is just determined by statistics and systematics.

4. CP violation and neutrino mass hierarchy

With the next generation of experiments discussed in the previous section we are entering the era of precision measurements, at the level of 1%. There are many ideas on how to go beyond this level, by performing high precision measurements with very intense beams aiming at several 100 kt size detectors at distances up

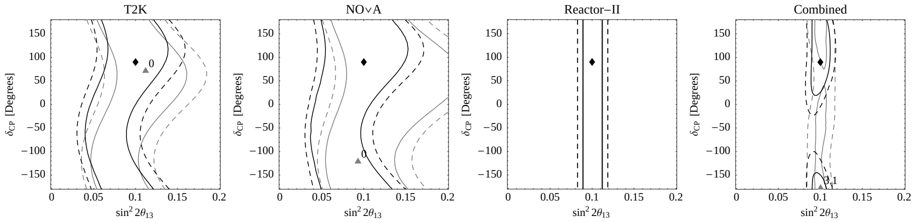

Figure 6. The 90% CL (solid) and 3σ (dashed) allowed regions (2 d.o.f.) in the $\sin^2 2\theta_{13}$–δ plane for the true values $\sin^2 2\theta_{13} = 0.1$ and $\delta = 90°$ for T2K, NOνA, a reactor experiment, and the combination. The black curves refer to the allowed regions for the normal mass hierarchy, whereas the gray curves refer to the inverted hierarchy. The best fits are marked as diamonds (normal hierarchy) and triangles (inverted hierarchy). For the latter, the $\Delta\chi^2$-value with respect to the best-fit point is also given [33].

to several 1000 km. These ideas include upgrades of superbeams or new neutrino sources like beta beams or neutrino factories. Such facilities will be able to address questions like leptonic CP violation or the type of the neutrino mass hierarchy, i.e. the sign of Δm^2_{31}. Currently many studies are being performed in order to identify optimal (or realistic) strategies towards these goals (see [42]). Figure 7, taken from that reference, shows the sensitivity to CP violation and the neutrino mass hierarchy for some examples of proposed facilities. Since both of these measurements crucially depend on the size of θ_{13}, the sensitivity is shown as a function of this parameter. The size of the bands in the figure (especially for the beta beam and the neutrino factory) shows that there are important experimental parameters which have to be understood in terms of feasibility and cost, which will affect the final physics performance. In the following I briefly comment on the physics behind these measurements.

CP violation in oscillations is induced by a complex phase in the mixing matrix, δ_{CP}. Being a generic three-flavour effect, CP violation vanishes for $\theta_{13} \to 0$. This can be immediately understood by considering the standard parametrization of the mixing matrix, where δ_{CP} appears always in combinations like $\sin\theta_{13} e^{i\delta_{CP}}$, and hence disappears for vanishing θ_{13} (see also eq. (3)). In principle, information on δ_{CP} can be obtained by comparing oscillation probabilities in CP conjugated oscillation channels, like $\nu_\mu \to \nu_e$ and $\bar{\nu}_\mu \to \bar{\nu}_e$. However, the matter effect (which is different for neutrinos and antineutrinos) leads in general to different transition probabilities, even if $\delta_{CP} = 0$. Therefore, the challenge is to disentangle intrinsic CP violation due to the complex mixing matrix from 'environmental' CP violation induced by the CP-odd matter traversed by the neutrino beam. The strategy is to perform a parametric fit using as much information as possible (e.g., spectral information) to extract δ_{CP} from data.

The key to resolve the type of the neutrino mass hierarchy is the matter effect [7,8] in $\nu_\mu \to \nu_e$ or $\nu_e \to \nu_\mu$ transitions due to θ_{13}. The crucial observation is that for $\Delta m^2_{31} > 0$ (normal hierarchy) there is a resonant enhancement of oscillations for neutrinos, whereas for $\Delta m^2_{31} < 0$ (inverted hierarchy) the resonance occurs for antineutrinos. Clearly, the matter effect becomes more important when more

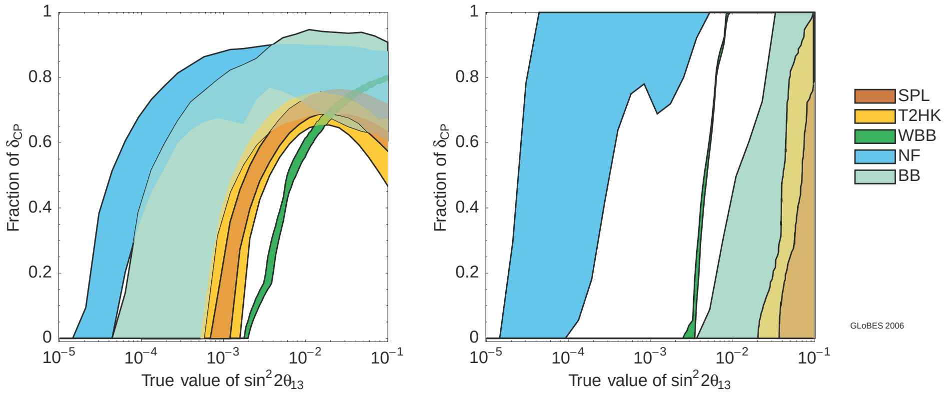

Figure 7. Fraction of values of the CP phase δ_{CP} for which CP violation (left) or the neutrino mass ordering (right) can be established, as a function of $\sin^2 2\theta_{13}$. The plots show the sensitivity of three examples for superbeams (SPL, T2HK, WBB), a neutrino factory (NF) and a beta beam (BB). The width of the bands corresponds to different assumptions on systematics as well as experimental configurations (see [42] for details).

matter is crossed. Therefore, one has to aim at long baselines in order to determine the mass hierarchy; the scale for 'long' is set in this context by noting that the matter effect becomes of order 1 for baselines of order 1000 km (see [43] for a recent discussion and references).

Acknowledgment

Support of the European Community-Research Infrastructure Activity under the FP6 'Structuring the European Research Area' program (CARE, contract number RII3-CT-2003-506395) is acknowledged.

References

[1] M Maltoni, T Schwetz, M A Tortola and J W F Valle, *Phys. Rev.* **D68**, 113010 (2003), hep-ph/0309130
[2] M Maltoni, T Schwetz, M A Tortola and J W F Valle, *New J. Phys.* **6**, 122 (2004), hep-ph/0405172v6
[3] MINOS: arXiv:0708.1495 [hep-ex] (2007)
[4] KamLAND: S Abe *et al*, arXiv:0801.4589 [hep-ex]
[5] KamLAND: T Araki *et al*, *Phys. Rev. Lett.* **94**, 081801 (2005), hep-ex/0406035
[6] SNO: B Aharmim *et al*, *Phys. Rev.* **C72**, 055502 (2005), nucl-ex/0502021
[7] L Wolfenstein, *Phys. Rev.* **D17**, 2369 (1978)
[8] S P Mikheev and A Y Smirnov, *Sov. J. Nucl. Phys.* **42**, 913 (1985)
[9] E Aliu *et al*, *Phys. Rev. Lett.* **94**, 081802 (2005), hep-ex/0411038
[10] SuperK: Y Ashie *et al*, *Phys. Rev.* **D71**, 112005 (2005), hep-ex/0501064

[10a] Small deviations from maximal mixing due to sub-leading three-flavour effects are discussed in [11,12]. At present such deviations are not statistically significant
[11] G L Fogli, E Lisi, A Marrone, A Palazzo and A M Rotunno, *Prog. Part. Nucl. Phys.* **57**, 71 (2006)
[12] M C Gonzalez-Garcia and M Maltoni, arXiv:0704.1800 [hep-ph] (2007)
[13] CHOOZ: M Apollonio *et al*, *Eur. Phys. J.* **C27**, 331 (2003), hep-ex/0301017
[14] S Goswami and A Y Smirnov, *Phys. Rev.* **D72**, 053011 (2005), hep-ph/0411359
[15] T Schwetz, *Phys. Scripta* **T127**, 1 (2006), hep-ph/0606060
[16] LSND: A Aguilar *et al*, *Phys. Rev.* **D64**, 112007 (2001), hep-ex/0104049
[17] MiniBooNE: A A Aguilar-Arevalo *et al*, *Phys. Rev. Lett.* **98**, 231801 (2007), arXiv:0704.1500 [hep-ex]
[18] KARMEN: B Armbruster *et al*, *Phys. Rev.* **D65**, 112001 (2002), hep-ex/0203021
[19] Y Declais *et al*, *Nucl. Phys.* **B434**, 503 (1995)
[20] F Dydak *et al*, *Phys. Lett.* **B134**, 281 (1984)
[21] S M Bilenky, C Giunti, W Grimus and T Schwetz, *Phys. Rev.* **D60**, 073007 (1999), hep-ph/9903454
[22] M Maltoni and T Schwetz, *Phys. Rev.* **D76**, 093005 (2007), arXiv:0705.0107 [hep-ph]
[23] M Maltoni, T Schwetz, M A Tortola and J W F Valle, *Nucl. Phys.* **B643**, 321 (2002), hep-ph/0207157
[24] M Sorel, J M Conrad and M Shaevitz, *Phys. Rev.* **D70**, 073004 (2004), hep-ph/0305255
[25] G Karagiorgi *et al*, *Phys. Rev.* **D75**, 013011 (2007), hep-ph/0609177
[26] S Goswami and W Rodejohann, *J. High Energy Phys.* **0710**, 073 (2007), arXiv:0706.1462 [hep-ph]
[26a] I would like to thank the authors of [26] for pushing for this check which finally has been completed during the WHEPP X workshop
[27] T Schwetz, *J. High Energy Phys.* **0802**, 011 (2008), arXiv:0710.2985 [hep-ph]
[28] T Schwetz, arXiv:0805.2234 [hep-ph] (2008)
[29] A Bandyopadhyay and S Choubey, arXiv:0707.2481 [hep-ph] (2007)
[30] S Choubey, arXiv:0709.1937 [hep-ph] (2007)
[31] A Donini, M Lusignoli and D Meloni, *Nucl. Phys.* **B624**, 405 (2002), hep-ph/0107231
[32] A Dighe and S Ray, arXiv:0709.0383 [hep-ph] (2007)
[33] P Huber, M Lindner, M Rolinec, T Schwetz and W Winter, *Phys. Rev.* **D70**, 073014 (2004), hep-ph/0403068
[34] T Kajita, these proceedings
[35] Double CHOOZ: F Ardellier *et al*, hep-ex/0606025
[36] Daya Bay: X Guo *et al*, hep-ex/0701029
[37] http://neutrino.snu.ac.kr/RENO/INTRO/intro.html
[38] T2K: Y Itow *et al*, hep-ex/0106019
[39] NOvA: D S Ayres *et al*, hep-ex/0503053.
[40] P Huber, M Lindner, T Schwetz and W Winter, *Nucl. Phys.* **B665**, 487 (2003), hep-ph/0303232
[41] M G Albrow *et al*, hep-ex/0509019 (2005)
[42] ISS Physics Working Group: A Bandyopadhyay *et al*, arXiv:0710.4947 [hep-ph]
[43] T Schwetz, *J. High Energy Phys.* **0705**, 093 (2007), hep-ph/0703279